Journal of Breast Imaging, 2021, 694–700
doi:10.1093/jbi/wbab073
Original Research
Received: June 4, 2021; Editorial Acceptance: August 31, 2021
Published Online: October 27, 2021

Original Research

Screening Digital Breast Tomosynthesis: Radiation Dose Among Patients With Breast Implants

Nhu Q. Vu, BS,[1] Curran Bice, MD,[1] John Garrett, PhD,[2] Colin Longhurst, MS,[3] Daryn Belden, BS,[2] Carolyn Haerr, MD, FACR,[2] Lucinda Prue, BA, RT (R) (M) (ARRT) (WI),[4] Ryan W. Woods, MD, MPH[1,2,*]

[1]University of Wisconsin, School of Medicine and Public Health, Madison, WI, USA; [2]UW Health, Department of Radiology, Madison, WI, USA; [3]University of Wisconsin, Department of Statistics, Madison, WI, USA; [4]UnityPoint Health-Meriter, Department of Radiology, Madison, WI, USA

*Address correspondence to R.W.W. (e-mail: rwoods@uwhealth.org)

Abstract

Objective: To compare the mean glandular dose (MGD), cancer detection rate (CDR), and recall rate (RR) among screening examinations of patients with breast implants utilizing various digital breast tomosynthesis (DBT)-based imaging protocols.

Methods: This IRB-approved retrospective study included 1998 women with breast implants who presented for screening mammography between December 10, 2013, and May 29, 2020. Images were obtained using various protocol combinations of DBT and 2D digital mammography. Data collected included MGD, implant type and position, breast density, BI-RADS final assessment category, CDR, and RR. Statistical analysis utilized type II analysis of variance and the chi-square test.

Results: The highest MGD was observed in the DBT only protocol, while the 2D only protocol had the lowest (10.29 mGy vs 5.88 mGy, respectively). Statistically significant difference in MGD was observed across protocols ($P < 0.0001$). The highest per-view MGD was among DBT full-field (FF) views in both craniocaudal and mediolateral oblique projections ($P < 0.0001$). No significant difference was observed in RR among protocols ($P = 0.17$). The combined 2D (FF only) + DBT implant-displaced (ID) views protocol detected the highest number of cancers (CDR, 7.2 per 1000), but this was not significantly different across protocols ($P = 0.48$).

Conclusion: The combination of 2D FF views and DBT ID views should be considered for women with breast implants in a DBT-based screening practice when aiming to minimize radiation exposure without compromising the sensitivity of cancer detection. Avoidance of DBT FF in this patient population is recommended to minimize radiation dose.

Key words: screening mammography; breast implants; radiation dose; digital breast tomosynthesis.

Introduction

Screening mammography is the gold standard for the early detection of breast cancer in asymptomatic women (1). However, exposure to ionizing radiation as part of screening breast exams may increase the risk for development of breast cancer (2). Radiation dose in mammography is determined by the mean glandular dose (MGD), defined as the average absorbed radiation dose over the at-risk fibroglandular breast tissue (3,4). The dose should be as low as possible without compromising the image quality needed for detecting

Key Messages

- A combination of 2D full-field views and digital breast tomosynthesis (DBT) implant-displaced views may be optimal in minimizing radiation dose in women with breast implants without significantly impacting recall rate or cancer detection rate in a DBT-based screening practice.
- Avoiding DBT full-field views in women with breast implants reduces radiation dose.

subtle lesions. Based on a recent review describing the radiation doses of different breast imaging technologies, the measured dose per view can vary widely across technologies and manufacturing systems, depending on several factors including compressed breast thickness and breast density (5). Digital breast tomosynthesis (DBT) was shown to have significantly higher doses than digital mammography (DM) (5). Another recent study demonstrated that compressed breast thickness was the greatest contribution to the radiation dose from screening mammography, followed by breast density, body mass index, and age (6).

For women without breast implants, the typical screening mammogram protocol includes bilateral craniocaudal (CC) and mediolateral oblique (MLO) projections. Women with breast implants also require implant-displaced (ID) views in CC and MLO projections. The additional ID views increase the amount of radiation delivered to each breast in exchange for visualization of more breast tissue. Breast augmentation is commonly performed for cosmetic or reconstruction purposes following mastectomy or lumpectomy for cancer. The American Society of Plastic Surgeons reported that breast augmentation has been a top cosmetic procedure since 2006, with at least 287 085 cases in 2019 (7). The potential risk of radiation-induced breast cancer from screening mammography will continue to increase in these patient populations, assuming that the number of women with breast implants will also continue to increase.

Historically, screening mammography only included 2D full-field (FF) DM views. However, 2D imaging is limited by tissue superimposition, making it difficult to distinguish true abnormalities from normal overlapping fibroglandular breast tissue (8). Digital breast tomosynthesis was developed in part to overcome this issue by creating a series of thin, reconstructed images of the breast, allowing for better visualization and localization of cancers (9). Currently, DBT-based screening exams may be performed on women with breast implants. However, the use of DBT is limited on FF views in these women. The American College of Radiology (ACR) suggests that DBT be performed only on ID views when used in combination with DM, as FF DBT views are limited in use due to artifacts created by the implant when synthesized imaging is being utilized (10). However, the ACR does not address the issue of differing radiation doses in this setting.

A previous large cohort study comparing the combination of DBT and 2D DM to DM alone demonstrated a 34% increase in overall cancer detection rate (CDR) and a 15.6% relative reduction in recall rate (RR) without an increase in false negative exams (11). Specific data on women with implants was not included in that study. However, the combination of DBT and DM for screening examination is associated with an increase in radiation dose compared with standard mammography screening (12). Concern about the increase in radiation dose caused by DBT was lessened by the introduction of synthesized 2D (s2D) mammography, a flat 2D image reconstructed from the DBT dataset. Synthesized 2D mammograms are used as substitution for standard 2D DM images in some practices. With this technique, patients are only exposed to radiation from the DBT component, decreasing the total radiation exposure by 39% to 45% (12–14).

To date, there is a lack of consensus on guidelines concerning mammography technique, suitable mammography quality criteria, and acceptable radiation doses for routine exams with breast implants (15). Several studies have published data on radiation dose in augmented breasts using DM (3,16,17). However, limited work has evaluated the radiation dose in DBT-based screening protocols among women with breast implants. The purpose of our study is to compare the MGD, CDR, and RR among screening exams of patients with breast implants, utilizing various imaging protocols that include a combination of DBT and 2D DM in routine clinical practice. We aim to provide a method for optimizing imaging for women with implants to minimize radiation exposure.

Methods

Study Design

This retrospective study was performed with institutional review board approval and was compliant with the Health Insurance Portability and Accountability Act.

Patients were identified using a language search of imaging reports that referenced the presence of breast implants. Imaging reports that did not describe the presence of an implant were excluded. The study population consisted of all women with silicone or saline implants who presented for routine screening mammography at our institution between December 10, 2013 and May 29, 2020. Women with breast implants for cosmetic purposes and reconstruction purposes following breast cancer surgery were included in this study. The distribution of cosmetic breast augmentation and reconstruction patients is assumed to be equal among the imaging protocols in this sample of consecutive screening mammograms. There were no other inclusion or exclusion criteria.

Imaging protocols were performed according to institutional protocols that were in place for patients with breast implants at the time of the exam. Each exam was reviewed to determine the number and types of views performed. In this study, the term FF is used for the full (non-ID) views.

Screening examinations were performed without (FF views) and with (ID views) displacement of the implant in CC and MLO projections, totaling at least four views per breast. Images were obtained using the following protocol combinations: (1) standard 2D DM only (all four views); (2) combined standard 2D DM for FF views, and DBT for ID views; (3) combined standard 2D DM for both ID and FF views, and DBT for ID views; (4) DBT only (all four views); and (5) other/nonstandard. For all protocols in which DBT images were obtained, the corresponding s2D image was also presented as part of the protocol.

All examinations were performed on the Hologic 3Dimensions (Hologic, Inc, Bedford, MA) or Selenia Dimensions 2D/3D (Hologic, Inc, Bedford, MA) Digital Mammography Systems, depending on the location patients presented to for screening mammography. All exams were performed by experienced certified mammography technologists. The imaging technique for implant exams is standardized such that all ID views are obtained using automatic exposure control (AEC) mode regardless of the protocol. In AEC mode, exposure parameters are automatically determined by the imaging equipment. Full-field images were acquired either by utilizing a manual technique set by the technologist such that the tube current (milliampere-seconds, mAs) and voltage (kiloelectron volt, keV) are set for each individual image according to recommended parameters based on compressed breast thickness, or by using AEC mode if there was adequate breast tissue anterior to the implant to be detected by the photo sensor cell on the equipment. The option for manual mode versus AEC mode was evaluated prior to the exam by the technologist, using previous images if they were available. The "Implant Present" setting on the Digital Imaging and Communications in Medicine (DICOM) header was set to "Yes" for all acquired images (both FF and ID views) in all study protocols. This setting is used independently of the AEC mode and solely for post-image capture processing purposes.

Data Collection

Mean glandular dose was automatically computed by the imaging system. For each patient, we collected the MGD for every DBT and 2D DM view from the study DICOM header. The radiation dose between DBT and 2D DM was then compared by per-view and per-breast analysis.

Chart review was performed and baseline characteristics were collected from the clinical records of the patients. These included implant type (silicone or saline), implant position (subglandular or submuscular), breast density, and the Breast Imaging Reporting and Data System (BI-RADS) final assessment category (18).

The overall CDR and RR were calculated for the exams included in each imaging protocol. The CDR was defined as the number of cancers (invasive carcinomas and ductal carcinomas in situ) diagnosed within 1 year of the date of the screening exam per 1000 screening exams. Cancers were identified by linking patient identifiers to a locoregional cancer registry. The RR was defined as the percentage of BI-RADS category 0 final assessments within each imaging protocol.

Statistical Analysis

Each individual patient was included more than once in our multilevel analyses. For exam-level analyses (eg, assessing variance in MGD), the statistical models included a random effect to adjust for the intra-patient correlation induced via the repeated measures structure of the data. However, the patient-level analyses (eg, assessing variance in CDR) were structured such that each patient only contributed one data point. Data from the patient-level analyses were independent and no random effects were necessary.

To assess the variance in MGD between DBT and 2D imaging across the four combinations of displacement variables and projection (ID/CC, ID/MLO, FF/CC, and FF/MLO), four linear mixed models were fit to the data using the "lme4" package (Version 1.1-26, Vienna, Austria). Each model was adjusted for body part thickness, implant type and position, age, and breast density. To adjust for the inter-patient correlation introduced via the repeated measurement design, the individual patient was modeled as a random intercept in each model. Approximate model *P* values were calculated using the Satterwhaite method, and the four *P* values of interest (comparing MGD between 2D and DBT) were corrected using the Bonferroni method.

To assess the per-breast variance of total MGD between the five exam workflows, a similar linear mixed model was fit to the data. The subsequent *P* value representing the between-workflow variability was calculated via a type II analysis of variance table (using the Satterwhaite approximation).

To assess the association between breast thickness and MGD, a linear mixed model was fit to the data where the individual patient was modeled as a random effect. Additionally, new linear mixed regression models were fit to the data to determine whether exposure control mode (AEC vs manual) had an impact on observed dose variance between 2D and DBT in the FF views.

The variability in RRs and CDRs between the different exam workflows were analyzed using chi-square tests. Subsequent 95% confidence intervals (CIs) about these proportions were estimated using the Agresti-Coull method. All statistical computations were done in R (Version 4.0.4, Madison, WI). A *P* value of less than 0.05 was considered statistically significant.

Results

The study population included 1998 women. The average patient age at the time of the exam was 55.3 years (SD, 9.2).

Imaging characteristics are detailed in Table 1. The average compressed breast thickness was 60.3 mm (SD, 24.4). Saline and silicone implants were approximately evenly distributed.

Among the 1998 patients, there was 1 patient in which the implant type was unknown and could not be reliably discerned from the images or clinical record, and 1 patient that had both subglandular and submuscular implant placement, one type in each breast. The distribution of breast composition resembles the distribution in an average population, with scattered fibroglandular and heterogeneously dense being the most common.

A total of 3649 exams including right or left breast images were evaluated in the study. The majority of exams were performed utilizing combined 2D and DBT imaging, as these imaging protocols have been in place at our institution for the greatest duration (Table 2).

Average MGD ranged from 5.9 to 10.8 mGy per breast across all protocols (Table 3). Among the standard imaging protocols, the DBT only protocol had the highest MGD whereas the 2D only protocol had the lowest MGD (10.3 mGy vs 5.9 mGy, respectively). A statistically significant difference in MGD was observed among all protocols ($P < 0.0001$). The highest per-view average MGD was among DBT FF views (Figure 1). Average MGD for DBT was significantly higher than 2D DM for both CC (3.1 mGy vs 1.5 mGy, respectively) and MLO projections (3.2 mGy vs 1.6 mGy, respectively).

The MGD was significantly higher for DBT than 2D DM in both CC and MLO projections in FF views ($P < 0.0001$). The difference in MGD between 2D and DBT in the CC projection in FF views was 1.6 mGy (95% CI: 1.4–1.6; $P < 0.0001$). When adjusted for exposure control mode (AEC versus manual), the difference was 1.4 mGy (95% CI: 1.3–1.5; $P < 0.0001$). In the MLO projection in FF views, the difference in MGD between 2D and DBT was 1.5 mGy (95% CI: 1.4–1.7; $P < 0.0001$). Similarly, in the exposure control mode–adjusted model, the difference was 1.5 mGy (95% CI: 1.4–1.6; $P < 0.0001$).

The average MGD for a standard 2D exam according to implant type and position was also evaluated. Interestingly, exams with saline implants had a higher average MGD than silicone implants (12.9 mGy vs 11.7 mGy, respectively; $P = 0.02$). The average MGD was 12.8 mGy for subglandular implants and 12.2 mGy for submuscular implants ($P < 0.001$). Although statistically significant, this difference is not likely to be clinically significant.

Additionally, average MGD was assessed between the four breast density categories and by compressed breast thickness. Although the entirely fatty breast group had the highest MGD (12.8 mGy), there was no statistically significant variation in average MGD for breast density ($P = 0.63$). There was a significant correlation between MGD and compressed breast thickness. A 1 unit increase in breast thickness was found to be associated with a 0.0035 increase in organ dose delivered (95% CI: 0.003–0.004; $P < 0.0001$).

Recall rate ranged from 0% to 4.6%, but no significant difference was observed in comparison between protocols ($P = 0.17$), implant type ($P = 0.54$), or implant position ($P = 0.65$).

Cancer detection varied by protocol. The combined 2D DM protocol that used 2D FF views in addition to DBT ID views detected 7.2 carcinomas per 1000 (95% CI: 3.7–13.4). The combined 2D DM protocol that used both 2D FF and 2D ID views in addition to DBT ID views detected 2.2 carcinomas per 1000 (95% CI: 0–13.9). Although these imaging protocols had a higher number of cancers detected,

Table 1. Imaging Characteristics of the Study Population ($N = 1998$)

Imaging characteristics	
Compressed breast thickness	*average ± SD (mm)*
All exams	60.3 ± 24.4
Full views	81.4 ± 13.2
ID views	40.5 ± 13.3
Implant type	*n* (%)
Saline	1019 (51.0%)
Silicone	978 (48.9%)
Unknown	1 (0.1%)
Implant position	*n* (%)
Subglandular	375 (18.8%)
Submuscular	1622 (81.2%)
Both, subglandular + submuscular	1 (0.1%)
Breast density	*n* (%)
Entirely fatty	52 (2.6%)
Scattered fibroglandular	944 (47.2%)
Heterogeneously dense	864 (43.2%)
Extremely dense	138 (6.9%)

Abbreviations: ID, implant-displaced; SD, standard deviation.

Table 2. Imaging Views and Number of Exams According to Protocol

Protocols	**No. of Exams ($N = 3649$)**[a]	**DBT ID**		**2D ID**	**DBT FF**	**2D FF**
2D only	41			X		X
Combined, 2D (FF only) + DBT ID	2853	X				X
Combined, 2D (FF+ID) + DBT ID	542	X		X		X
DBT only	177	X			X	
Other/non-standard	36	X	or	X	X	X

Abbreviations: DBT, digital breast tomosynthesis; FF, full-field; ID, implant-displaced.
[a]The number of exams includes right and left breasts as individual exams.

Table 3. Comparison of Radiation Dose and Screening Performance Parameters Between Protocols

Protocols	MGD per Breast, mGy (95% CI)[a]	Recall Rate, % (95% CI)	Cancer Detection Rate, *n*/1000 (95% CI)
2D only	5.9 (9.6–12.0)	4.2 (0–22.0)	0 (0–163)
Combined, 2D (FF only) + DBT ID	6.2 (6.1–6.3)	4.6 (3.6–5.8)	7.2 (3.7–13.4)
Combined, 2D (FF+ID) + DBT ID	7.5 (7.3–7.7)	3.1 (1.8–5.2)	2.2 (0–13.9)
DBT only	10.3 (9.8–10.8)	0 (0–4.3)	0 (0–43.2)
Other/non-standard	10.8 (9.6–12.0)	3.2 (0–17.6)	0 (0–131)
P-value	0.0001	0.17	0.48

Abbreviations: CI, confidence interval; DBT, digital breast tomosynthesis; FF, full-field; ID, implant-displaced; MGD, mean glandular dose.
[a]MGD per breast refers to the average MGD per breast across all patients.

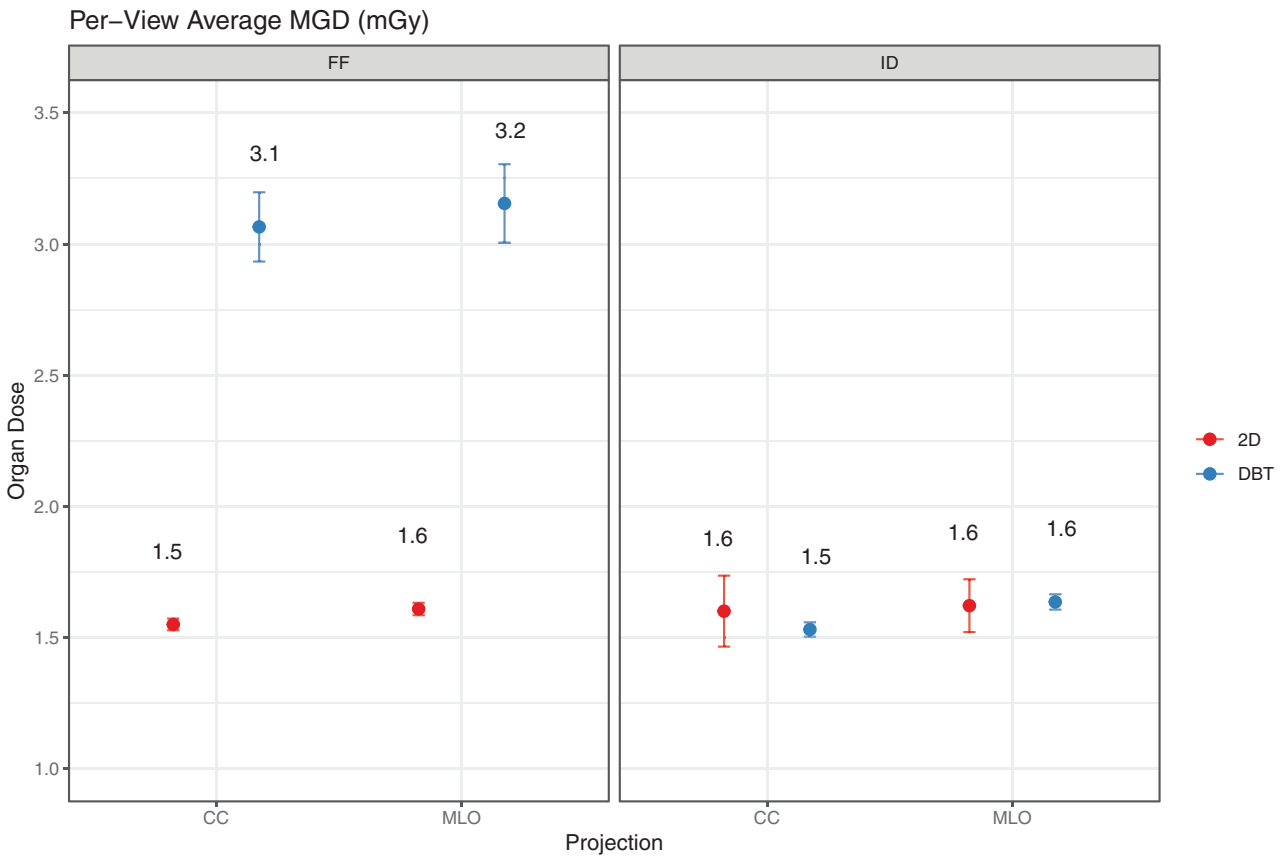

Figure 1. Average mean glandular dose (MGD) with 95% confidence intervals on craniocaudal (CC) and mediolateral oblique (MLO) projections per view for full-field (FF) and implant-displaced (ID) views using 2D digital mammography and digital breast tomosynthesis (DBT).

there was no statistically significant difference in CDR across protocols (P = 0.48). There was also no statistically significant difference in CDR by implant type (P = 0.23), implant position (P = 0.06), or breast density (P = 0.82).

Discussion

In our study, we demonstrated that among women with implants undergoing screening mammography, imaging protocols that included DBT had the highest average MGD, while the protocol limited to 2D views had the lowest. The increase in MGD among DBT-based protocols is largely attributed to the usage of DBT for FF views in either the CC or MLO projections with the implant in view. The ACR Practice Parameter for the Performance of Screening and Diagnostic Mammography states that DBT is typically only performed on ID views due to its limited utility on FF views (1). Our study also supports this practice based on the lower radiation dose in ID views when DBT is used.

Women with implants receive a higher radiation dose than women without breast implants during screening exams for two primary reasons. First, a greater number of images

are acquired to include both FF and ID views in CC and MLO projections, which increases the total radiation dose. Second, the presence of implants increases the breast thickness, and the dense implant requires increased radiation dose for each view to penetrate the implant and create a higher quality image for interpretation.

In addition, DBT has a higher MGD than standard 2D mammography. The dose is particularly increased compared to standard 2D mammography when the imaging protocol requires the technologist to acquire both DBT images in the ID views and standard 2D images in both FF and ID views (the combined 2D (FF+ID) + DBT ID views protocol in our study). The additional DBT images significantly raise the average MGD compared to 2D alone. In our study, we also demonstrated statistically higher average MGD with saline implants and implants in the subglandular position, although the absolute difference in radiation dose has limited clinical significance.

The current literature regarding radiation dose in women with implants is focused on primarily 2D imaging examinations. To our knowledge, our study is one of the first to evaluate radiation dose in DBT-based screening protocols in women with breast implants. A recent prior study evaluating MGD among women with implants undergoing 2D DM screening demonstrated higher median MGD for standard views compared to ID views, and that implant position does not affect MGD (3). In contrast to the results from this previous study, our study found subglandular implants to have a higher MGD compared to submuscular implants in a standard 2D exam, although the absolute difference is not likely to be meaningful.

Finally, while the 2D only protocol had the lowest average MGD, the combined 2D (FF only) + DBT ID views protocol had the highest number of cancers detected, although the CDR was not statistically significant among protocols. Based on our results and the many studies demonstrating increased cancer detection with DBT screening (11,19–22), we support the use of the combination of 2D FF views and DBT ID views in women with breast implants as this imaging protocol takes advantage of the benefits of DBT, which include optimizing cancer detection while minimizing the radiation dose delivered. Although the differences in RR and CDR across imaging protocols were not found to be significant in our study, the statistical power to detect such differences is limited due to our relatively small sample size. Further investigation is required to confirm our findings.

There are several limitations to our study. First, MGD data was collected directly from the DICOM header. The algorithm for calculating organ dose from vendors is generally performed on an implant-free model, which may not be representative of the true absorbed radiation dose and could impact our study results. A recent study reported a MGD difference up to 0.67 mGy between the displayed organ dose in Hologic systems and the calculated dose (23). This small difference could have practical implications in clinical practice if the true absorbed dose exceeds the accepted dose level. Previous studies have found different MGD values across various breast thickness levels in women with silicone implants, with no obvious consensus (16,24). Thus, there is a need for better models to accurately assess the dose in an augmented breast. Second, because our study included both cosmetic breast augmentation patients and implant-based breast reconstruction patients, the risk of malignancy in our study population may be higher than in a population of women who underwent breast augmentation solely for cosmetic reasons; this may impact RR or CDR.

Conclusion

In summary, our study demonstrates that the combination of 2D FF views and DBT ID views should be considered for women with breast implants in a DBT-based screening practice when the goal is to minimize radiation exposure without compromising the sensitivity of cancer detection. Larger studies are required to assess the differences in RR and CDR between various DBT-based screening protocols for women with breast implants in order to establish a clear optimal imaging protocol. Avoidance of FF DBT views in patients with implants is recommended to reduce radiation dose while maintaining screening performance.

Funding

None declared.

Conflict of Interest Statement

None declared.

References

1. *American College of Radiology*. American College of Radiology practice parameter for the performance of screening and diagnostic mammography. Available at: https://www.acr.org/-/media/ACR/Files/Practice-Parameters/screen-diag-mammo.pdf. Accessed August 21, 2021.
2. Lin EC. Radiation risk from medical imaging. *Mayo Clin Proc* 2010;85(12):1142–1146.
3. Couto LS, Freitas-Junior R, Correa RS, et al. Mean glandular dose in digital mammography in women with breast implants. *J Radiol Prot* 2019;39(2):498–510.
4. Bouwman RW, van Engen RE, Young KC, et al. Average glandular dose in digital mammography and digital breast tomosynthesis: comparison of phantom and patient data. *Phys Med Biol* 2015;60(20):7893–7907.
5. Hendrick RE. Radiation doses and risks in breast screening. *J Breast Imaging* 2020;2(3):wbaa016. doi:10.1093/jbi/wbaa016.
6. Nguyen JV, Williams MB, Patrie JT, Harvey JA. Do women with dense breasts have higher radiation dose during screening mammography? Reply to-Letter to the Editor. *Breast J* 2018;24(4):708.

7. *American Society of Plastic Surgeons*. Plastic surgery statistics report 2019. Available at: https://www.plasticsurgery.org/documents/News/Statistics/2019/plastic-surgery-statistics-report-2019.pdf. Accessed September 22, 2021.
8. Vedantham S, Karellas A, Vijayaraghavan GR, Kopans DB. Digital breast tomosynthesis: state of the art. *Radiology* 2015;277(3):663–684.
9. Ortenzia O, Rossi R, Bertolini M, Nitrosi A, Ghetti C. Physical characterisation of four different commercial digital breast tomosynthesis systems. *Radiat Prot Dosimetry* 2018;181(3):277–289.
10. *American College of Radiology*. American College of Radiology practice parameter for the performance of digital breast tomosynthesis (DBT). Available at: https://www.acr.org/-/media/ACR/Files/Practice-Parameters/DBT.pdf?la=en. Accessed August 21, 2021.
11. Conant EF, Beaber EF, Sprague BL, et al. Breast cancer screening using tomosynthesis in combination with digital mammography compared to digital mammography alone: a cohort study within the PROSPR consortium. *Breast Cancer Res Treat* 2016;156(1):109–116.
12. Svahn TM, Houssami N, Sechopoulos I, Mattsson S. Review of radiation dose estimates in digital breast tomosynthesis relative to those in two-view full-field digital mammography. *Breast* 2015;24(2):93–99.
13. Skaane P, Bandos AI, Eben EB, et al. Two-view digital breast tomosynthesis screening with synthetically reconstructed projection images: comparison with digital breast tomosynthesis with full-field digital mammographic images. *Radiology* 2014;271(3):655–663.
14. Zuckerman SP, Maidment ADA, Weinstein SP, McDonald ES, Conant EF. Imaging with synthesized 2D mammography: differences, advantages, and pitfalls compared with digital mammography. *AJR Am J Roentgenol* 2017;209(1):222–229.
15. Sá dos Reis C, Gremion I, Richli Meystre N. Study of breast implants mammography examinations for identification of suitable image quality criteria. *Insights Imaging* 2020;11(1):3.
16. Beckett JR, Kotre CJ. Estimation of mean glandular dose for mammography of augmented breasts. *Phys Med Biol* 2000;45(11):3241–3252.
17. Smathers RL, Boone JM, Lee LJ, Berns EA, Miller RA, Wright AM. Radiation dose reduction for augmentation mammography. *AJR Am J Roentgenol* 2007;188(5):1414–1421.
18. D'Orsi CJ, Sickles EA, Mendelson EB, Morris EA, et al. *ACR BI-RADS® Atlas, Breast Imaging Reporting and Data System*. Reston, VA: American College of Radiology; 2013.
19. Skaane P, Bandos A, Gullien R, et al. Comparison of digital mammography alone and digital mammography plus tomosynthesis in a population-based screening program. *Radiology* 2013;267(1):47–56.
20. Ciatto S, Houssami N, Bernardi D, et al. Integration of 3D digital mammography with tomosynthesis for population breast-cancer screening (STORM): a prospective comparison study. *Lancet Oncol* 2013;14(7):583–589.
21. Bernardi D, Macaskill P, Pellegrini M, et al. Breast cancer screening with tomosynthesis (3D mammography) with acquired or synthetic 2D mammography compared with 2D mammography alone (STORM-2): a population-based prospective study. *Lancet Oncol* 2016;17(8):1105–1113.
22. McDonald ES, Oustimov A, Weinstein SP, Synnestvedt MB, Schnall M, Conant EF. Effectiveness of digital breast tomosynthesis compared with digital mammography: outcomes analysis from 3 years of breast cancer screening. *JAMA Oncol* 2016;2(6):737–743.
23. Suleiman ME, Brennan PC, McEntee MF. Mean glandular dose in digital mammography: a dose calculation method comparison. *J Med Imaging (Bellingham)* 2017;4(1):013502.
24. Cassola VF, Hoff G. Monte Carlo study of glandular dose distribution on radiological procedures for woman who has breast silicone implant. *IEEE Nuclear Science Symposium Conference Record* 2009. doi:10.1109/NSSMIC.2009.5402097.